

## Tumorigenesis and Neoplastic Progression

# Tumorigenic Role of Orphan Nuclear Receptor NR0B1 in Lung Adenocarcinoma

Tomofumi Oda,<sup>\*†</sup> Tian Tian,<sup>\*†</sup> Masayoshi Inoue,<sup>†</sup>  
Jun-ichiro Ikeda,<sup>\*</sup> Ying Qiu,<sup>\*\*†</sup>  
Meinoshin Okumura,<sup>†</sup> Katsuyuki Aozasa,<sup>\*</sup>  
and Eiichi Morii<sup>\*</sup>

From the Departments of Pathology<sup>\*</sup> and General Thoracic Surgery,<sup>†</sup> Osaka University, Graduate School of Medicine, Osaka, Japan; and the Department of Pathology,<sup>‡</sup> Tongji University School of Medicine, Shanghai, China

**Cancer stem cells are a limited population of tumor cells that are thought to reconstitute whole tumors. The Hoechst dye exclusion assay revealed that tumors are composed of both a main population and a side population of cells, which are rich in cancer stem cells. NR0B1 is an orphan nuclear receptor that is expressed to a greater extent in the side population, as compared with the main population, of a lung adenocarcinoma cell line. In this study, we investigated the role of NR0B1 in lung adenocarcinoma cells. Reduction of NR0B1 expression levels in lung adenocarcinoma cell lines resulted in vulnerability to anti-cancer drugs and decreased abilities for invasion, *in vitro* colony formation, and tumorigenicity in non-obese diabetic/severe compromised immunodeficient mice. When 193 cases of lung adenocarcinoma were immunohistochemically examined, higher levels of NR0B1 expression correlated with higher rates of lymph node metastasis and recurrence. Multivariate analysis revealed high NR0B1 expression levels, stage of the disease, and size of tumor to be independent unfavorable prognostic factors for overall and disease-free survival rates. In clinical samples, NR0B1 expression levels inversely correlated to the proportion of methylated CpG sequences around the transcription initiation site of the NR0B1 gene, suggesting the epigenetic control of NR0B1 transcription in lung adenocarcinoma. In conclusion, NR0B1 might play a role in the malignant potential of lung adenocarcinoma. (Am J Pathol 2009, 175:1235–1245; DOI: 10.2353/ajpath.2009.090010)**

Cancer cells comprise heterogeneous groups of cells; only a small population of cancer cells possesses the

ability to reconstitute whole tumor.<sup>1–3</sup> This population, called cancer stem cells (CSCs), efficiently forms colonies in semisolid culture and is xenotransplantable in non-obese diabetic/severely compromised immunodeficient (NOD/SCID) mice.<sup>4</sup> CSCs were first identified in leukemia,<sup>5,6</sup> and subsequently isolated from the solid tumors, such as breast, brain, prostate, colon, pancreatic, and head/neck cancers.<sup>7–13</sup> CSCs highly express various chemical transporters and could efficiently efflux several chemicals, which might render to resistance to anti-cancer drugs and tumor recurrence.<sup>4,14,15</sup>

Efficient dye-efflux ability could be used for the isolation of CSCs. Most cancer cells are stained intensely with the fluorescent dye Hoechst 33342, whereas cancer cells with stem cell properties are not.<sup>4,14,15</sup> At flow-cytometry analysis, cells with a low level of Hoechst 33342 are visualized as a faintly stained population, which is called the side-population (SP).<sup>16</sup> Only the SP gives rise to both SP and non-SP (the main population, hereafter called MP), and the SP, but not MP, is tumorigenic in NOD/SCID mice.<sup>17</sup> These findings support the notion that CSCs are enriched in the SP. Recently, the presence of SP was reported in cancer cell lines established from various tumors, such as glioma, mammary carcinoma, and lung cancer.<sup>18–20</sup> Proteins highly expressed in the SP may become the candidate of CSC markers.

Lung cancer has become the most common cause of cancer death worldwide since 1985, and the annual mortality was 1.18 million peoples in the world.<sup>21</sup> Despite the advances in the methods for detection and treatment of lung cancer, its prognosis still remains unfavorable. Remnant tumor cells resistant to anti-cancer drugs may provide a basis for recurrence after chemotherapy. In this context, evaluation of lung cancers from the standpoint of CSCs may be important. To date, however, any markers useful for detection of CSCs in lung cancer have not been known. Recently, Seo et al<sup>22</sup> reported that several genes

---

Supported by grants from the Ministry of Education, Culture, Sports, Science and Technology, Japan.

There is no conflict of interest in this study.

Accepted for publication May 21, 2009.

Address reprint requests to Eiichi Morii, M.D., Department of Pathology, Graduate School of Medicine, Osaka University, Yamada-oka 2-2, Suita 565-0871, Japan. E-mail: morii@patho.med.osaka-u.ac.jp.

were highly expressed in SP of lung adenocarcinoma cell lines: one of them was the gene for NR0B1, a recently characterized member of the orphan nuclear receptor family.<sup>23</sup> NR0B1 (also called dosage-sensitive sex reversal/adrenal hypoplasia congenital critical region on the X chromosome 1; DAX1) acts as a negative regulator of steroid production, and is expressed in the reproductive and endocrine systems.<sup>23</sup> A recent study on the embryonic stem cells showed that NR0B1 is abundantly expressed in an undifferentiated status, but its expression level is down-regulated on differentiation.<sup>24</sup> Knocked down of NR0B1 expression resulted in differentiation of embryonic stem cells, suggesting a role of NR0B1 for the maintenance of undifferentiated state.<sup>25</sup>

NR0B1 is expressed in several kinds of cancers, such as endometrial carcinoma, ovarian carcinoma, prostatic carcinoma, and Ewing's sarcoma.<sup>26-30</sup> Recently, Mendiola et al<sup>29</sup> and Kinsey et al<sup>30</sup> reported that NR0B1 was a target of EWS/FLI fusion protein in Ewing's sarcoma: knocked-down expression of NR0B1 in the Ewing's sarcoma cell lines resulted in the defect of colony formation ability and tumorigenicity. These findings suggested that NR0B1 expression could be a marker for tumorigenic cells in lung adenocarcinoma, as well as Ewing's sarcoma. To date, there have not been any reports describing the expression and role of NR0B1 in lung adenocarcinoma. In the present study, the role of NR0B1 was investigated in lung adenocarcinoma cell line, and subsequently, the clinicopathological features between lung adenocarcinoma with high and low expression level of NR0B1 were compared. In addition, the epigenetic regulation mechanism of NR0B1 gene transcription was investigated.

## Materials and Methods

### Cells and Flow Cytometry

The human lung adenocarcinoma cell lines A549 and PC-14 were purchased from the American Type Culture Collection (Rockville, MD) and the Riken Bioresource Center (Tsukuba, Japan), respectively. Cells were cultured in Dulbecco's Modified Eagle's Medium (DMEM, Sigma, St Louis, MO) supplemented with 10% fetal calf serum (FCS; Nippon Bio-supp. Center, Tokyo, Japan; DMEM-10% FCS). SP analysis was performed according to the protocol of Goodell's laboratory with minor modifications.<sup>16</sup> Briefly, cells ( $1 \times 10^6$ /ml) were incubated at 37°C for 90 minutes with 5  $\mu$ g/ml Hoechst 33342 (Sigma) with or without 50  $\mu$ mol/L verapamil (Sigma), collected and resuspended in ice-cold PBS with 2% FCS and 2  $\mu$ g/ml propidium iodide (BD Pharmingen, San Diego, CA). SP and MP cells were analyzed and sorted with fluorescence-activated cell sorting-Vantage (Becton Dickinson, BD, Franklin Lakes, NJ) carrying a triple-laser. The Hoechst 33342 was excited with the UV laser at 350 nm, and fluorescence emission was measured with 424/BP44 (Hoechst blue) and 660/BP20 (Hoechst red) optical filters.

### Quantification of mRNA Levels by Real-Time Reverse-Transcription PCR

RNA was extracted using an RNeasy kit (Qiagen, Valencia, CA) with DNase I treatment. Total RNA was subjected to reverse transcription (RT) by Superscript III (Invitrogen, Carlsbad, CA), and the single strand cDNA was obtained. The mRNA levels for NR0B1, B cell/chronic lymphocytic leukemia lymphoma (Bcl)-2, matrix metalloproteinase (MMP)-2, and glyceraldehyde-3-phosphate dehydrogenase (GAPDH) genes were verified using TaqMan gene expression assays (Applied Biosystems, Foster City, CA) as recommended by the manufacturer. The amount of NR0B1, Bcl-2, and MMP-2 mRNA was normalized to that of GAPDH mRNA, and the normalized value was shown as relative mRNA amount.

### Semiquantitative RT-PCR Analysis

The reverse-transcribed product (1 or 0.1  $\mu$ l) was added to 25  $\mu$ l of a PCR mixture containing 1.25 U of TaqDNA polymerase (Roche Diagnostics GmbH, Mannheim, Germany) and 25 pmol of each primer. The sequences of the primers were: 5'-CGACTTCGCCGAGATGTCCAGCCAG-3' and 5'-ACTTGTGGCCCAGATAGGCACCCAG-3' for Bcl-2, 5'-GGACCCGGTGCCTCAGGA-3' and 5'-CAAAGATGGTCA-CGGTCTGC-3' for BclII-associated x (Bax), 5'-TTGGA-CAATGGACTGGTTGA-3' and 5'-GTAGAGTGGATGGT-CAGTG-3' for Bcl-X<sub>L/S</sub>, 5'-AGATCTTCTTCTCAAGGAC-CGGTT-3' and 5'-GGCTGGTCAGTGGCTTGGGGTA-3' for MMP-2, 5'-TTGCGCCATCTACAGGAG-3' and 5'-ACT-GGGGATCGTTATACATC-3' for urokinase-type plasminogen activator (uPA), 5'-TGCATGCAGTGTAAGACC-3' and 5'-CTGCGGCAGATTTTCAAG-3' for uPA receptor, 5'-ATC-CTGTTGTTGCTGTGGCTGATAG-3' and 5'-TGCTGGGTG-GTAACTCTTTATTTCA-3' for tissue inhibitor of metalloproteinase (TIMP)-1, 5'-TTTATCTACACGGCCCCCTCCTCAG-3' and 5'-ACGGGTCTCGATGTCAAGAACTC-3' for TIMP-2, and 5'-GTCCACTGGCGTGTTCACCA-3' and 5'-GTG-GCAGTGATGGCATGGAC-3' for GAPDH.

### Knocked Down of NR0B1 Expression by Small Interfering RNA

To generate a stably expressing small interfering (si)-RNA system, the BLOCK-iT Pol II miR RNAi expression vector kit (Invitrogen) was used. Cells stably expressing the NR0B1 si-RNA and control cells stably expressing vector alone were established in DMEM-10% FCS containing blasticidin S (Invivogen) at a concentration of 10  $\mu$ g/ml in A549 and 12  $\mu$ g/ml in PC-14.

### Immunoblotting

Cells were harvested, and the whole cell lysates were prepared as described previously.<sup>31</sup> The lysates were separated on 10% SDS-polyacrylamide gels, transferred to Immobilon (Millipore, Bedford, MA), and incubated with anti-NR0B1 (Abcam Ltd, Cambridge, UK) or anti-

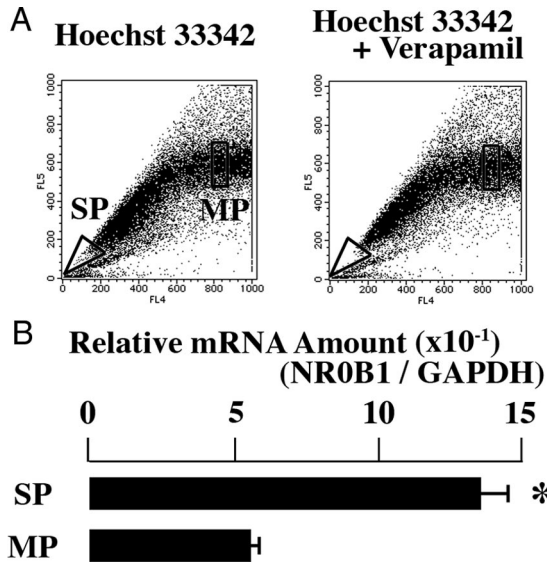


**Figure 1.** High NR0B1 expression in SP of A549. **A:** Dot blot analysis of A549 cells stained with Hoechst 33342 dye in the absence (**left**) or presence (**right**) of verapamil. SP and MP cells were boxed. **B:** Quantitative real-time RT-PCR was performed with mRNA obtained from SP and MP of A549. The amount of NR0B1 mRNA was normalized for the amount of GAPDH mRNA. The values represent the mean  $\pm$  SE of three experiments. \* $P < 0.01$  by the Student's *t*-test.

actin (Sigma) antibodies. After washing, the blots were incubated with an appropriate peroxidase-labeled secondary antibody (MBL, Nagoya, Japan), and then reacted with Renaissance reagents (NEN, Boston, MA) before exposure.

*Cell Proliferation Assay*

Cell growth of A549 was shown by number of cells. Approximately  $1 \times 10^4$  cells were seeded onto cell culture plates

with DMEM-10% FCS. The growth medium was changed every 2 days and cell numbers were counted.

*Assessment of Anti-Cancer Drug Topotecan Effect*

Topotecan acts as a topoisomerase I inhibitor, and induces apoptosis in tumor cells.<sup>32</sup> The effect of topotecan was evaluated as described by Tomicic et al<sup>33</sup> with minor modification. Briefly, cells ( $1 \times 10^4$ ) were seeded onto cell culture plates with DMEM-10% FCS, cultured for 12 hours, and then various concentration of topotecan (LKT Laboratories Inc, St Paul, MN) was added. After 12 hours, the viability of cells was assessed with Premix WST-1 cell assay system (Takara Bio Inc, Kyoto, Japan). The absorbance at 450 nm was divided by that obtained in the cells without topotecan, and the resultant value was shown as viability index.

*Matrigel Invasion Assay*

Invasion of tumor cells into the Matrigel was examined with BD BioCoat Matrigel Invasion Chamber (BD Biosciences, San Jose, CA). Briefly, cells were seeded in DMEM without FCS on the Matrigel invasion chamber, and cultured in DMEM-10% FCS for 30 hours. Invading cells were stained with Diff-quick staining kit (Siemens, Munich, Germany). Number of invading cells was counted at five microscopic fields per well at a magnification of  $\times 100$ , and the extent of invasion was expressed as the average number of cells per  $\text{mm}^2$ .

*In Vitro Colony Formation Assay*

Cells were suspended in a volume of 0.1 ml of DMEM-10% FCS, and 500 cells were plated in culture dishes

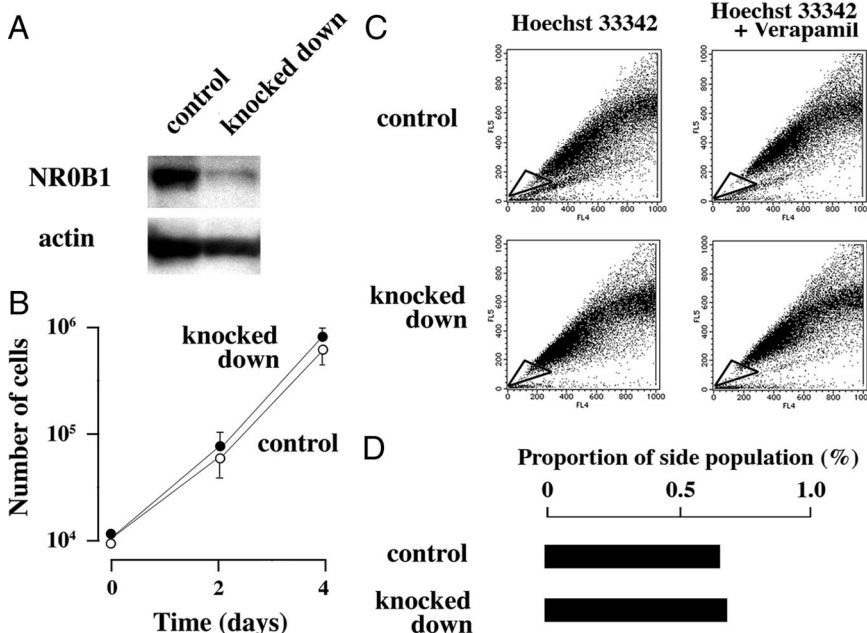


**Figure 2.** Effect of NR0B1 expression on the proliferative activity and the SP formation. **A:** Immunoblot analysis for the amount of NR0B1 protein in the control and si-RNA knocked down cells. **B:** Comparison of cell proliferation of NR0B1 knocked down cells to that of control cells. The values represent the mean  $\pm$  SE of three experiments. **C:** Dot blot analysis of control (**upper**) and knocked down (**lower**) cells stained with Hoechst 33342 dye in the absence (**left**) or presence (**right**) of verapamil. SP cells were boxed. **D:** Proportion of SP in the control and knocked down cells.

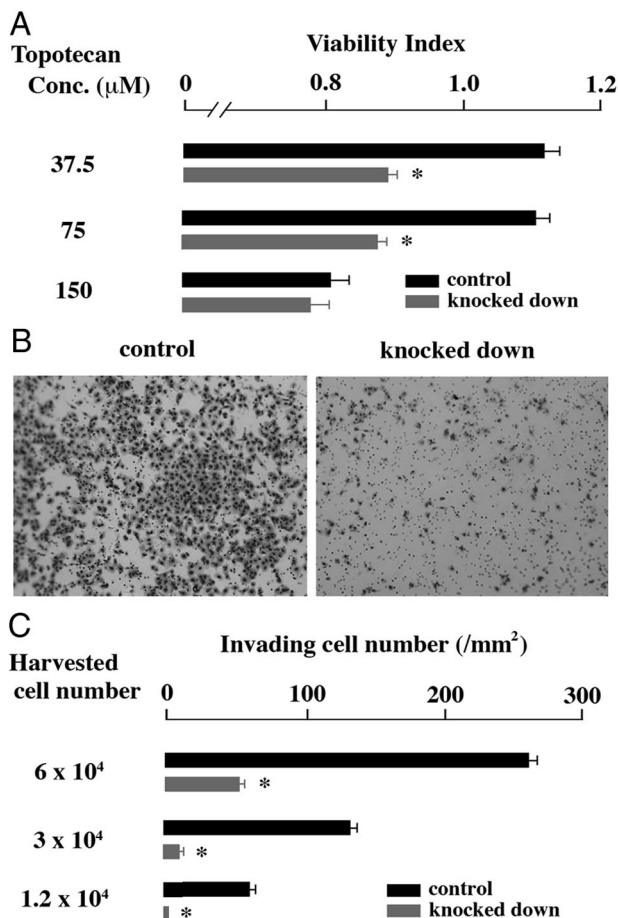


**Figure 3.** Effect of NROB1 expression on the resistance against topotecan and the cell invasion activity. **A:** Viability in the presence of various amount of topotecan was compared. **B:** Matrigel invasion assay. Cells invading through Matrigel are shown. Original magnification, ×100. **C:** Invading cell number per mm<sup>2</sup>. The values shown in (A) and (C) are the mean ± SE of three experiments. \**P* < 0.01 by the Student's *t*-test.

with 1 ml of methylcellulose-containing DMEM supplemented with 15% FCS. The number of colonies was counted on day14.

### Mice and Xenograft Transplantation

Six-to 8-week-old female NOD/SCID mice were purchased from Charles River Laboratories Japan (Kanagawa, Japan) and kept under specific pathogen-free conditions. Before xenotransplantation, the mice were deeply anesthetized. All animal experiments were performed according to the guideline of Osaka University Animal Center, and approved by the institutional review board of committee of animal experiments (No. 753). For xenograft transplantation, cells ( $1 \times 10^4$ ) were suspended in 0.2 ml of Matrigel (BD Biosciences), and were injected subcutaneously into NOD/SCID mice. The tumor volume was estimated using the following formula:  $(\text{width})^2 \times (\text{length})/2$  according to the report by Meyer-Siegler et al.<sup>34</sup>

### In Vitro Methylation

The luciferase construct that contained promoter region of NROB1 starting from nt -474<sup>35</sup> was incubated with

SssI methylase (New England Biolabs, Beverly, MA) in the presence (methylated) or absence (mock) of S-adenosylmethionine, as recommended by the manufacturer. After DNA isolation, 1 μg of the methylated or mock luciferase construct was transiently transfected into A549, together with 0.2 μg of the pRL-TK containing Renilla luciferase gene (Promega, Madison, WI) using Transfast transfection reagent (Promega). Forty-eight hours after transfection, the luciferase activity was measured by Dual Luciferase Reporter Assay Kit (Promega).

### Bisulfite Modification and DNA Sequencing Analysis

One μg of genomic DNA was modified with sodium bisulfite using EpiTect Bisulfite Kit (Qiagen), and used for PCR as a template. The PCR reaction mixture contained 1 μl of DNA in a total volume of 25 μl, 2.5 μl of 10× PCR buffer II, 5 μmol/L MgCl<sub>2</sub>, 250 μmol/L deoxynucleoside triphosphate, 1 μmol/L of each primer, and 1.25units Taq gold. The PCR buffer II, MgCl<sub>2</sub>, and Taq gold are parts of the AmpliTaq Gold with Gene Amp kit (Applied Biosystems). Sequence of the primers was as follows; 5'-AGGAAAGT-GTTTAGGAGTTTTT and 5'-CCTAAAACCTATTTTATAC-CT. The PCR was done at 95°C for 10 minutes, followed by 40 cycles at 95°C for 1 minute, 51°C for 1 minute, and 72°C for 1 minute. In this condition, equal number of clones was obtained for samples with methylated and unmethylated NROB1 promoter when equal amount of clone was mixed. Amplified PCR fragments were purified with QIAquick gel extraction kit (Qiagen), and was subcloned into pGEM-T Easy vector (Promega). The sequences of the amplified fragments were analyzed using an ABI 3100 sequencer (Applied Biosystems).

### Patients

A total of 193 patients who underwent surgery for lung adenocarcinoma at Osaka University Hospital during the period from January 1993 to January 2004 were examined. The histological stage was determined according to the sixth edition of the Union International Contre le Cancer—TNM staging system.<sup>36</sup> Histological specimens were fixed in 10% formalin and routinely processed for paraffin embedding. Paraffin-embedded specimens were stored in the dark room in the Department of Pathology of Osaka University Hospital at room temperature, and were sectioned at 4 μm thickness at the time of staining. All patients were followed up with laboratory examinations including routine peripheral blood cell counts at 1- to 6-month intervals, chest roentgenogram, computed tomographic scan of the chest, and endoscopic examinations of the bronchus at 6- to 12-month intervals. The follow-up period for survivors ranged from 5 to 150 (median, 61) months. The mRNA and genomic DNA were obtained from several tumor samples, and stocked in -80°C. The study was approved by the ethical review board of Graduate School of Medicine, Osaka University (No. 737).

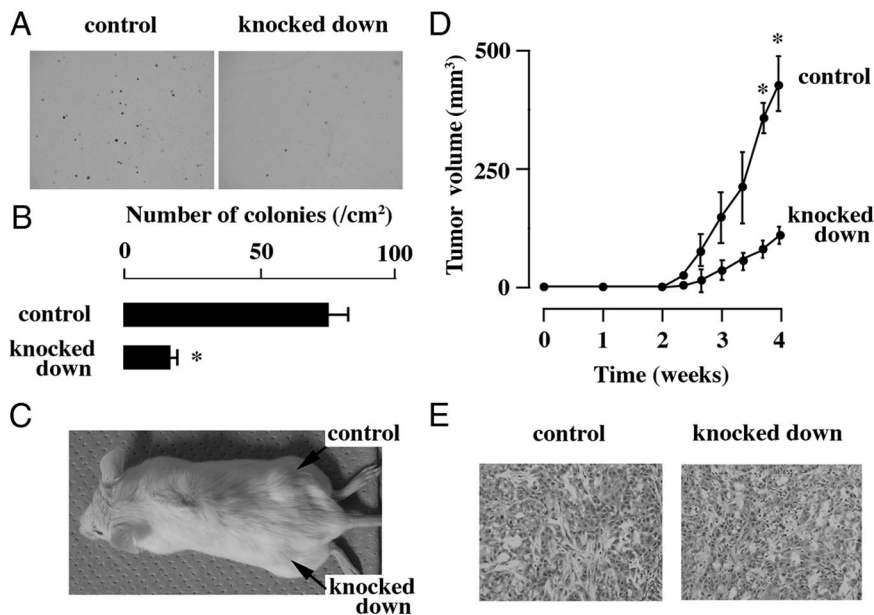


**Figure 4.** Effect of NR0B1 on the *in vitro* colony formation and the *in vivo* tumorigenicity activities. **A:** Colonies derived from the control and the NR0B1 knocked down cells. Original magnification,  $\times 40$ . **B:** Number of colonies per cm<sup>2</sup>. **C:** Tumors in NOD/SCID mice at the injection sites of the control and the knocked down cells. **D:** The change of the volume of tumors. **E:** Histology of tumors derived from the control and the knocked down cells. Original magnification,  $\times 400$ . The values in (B) and (D) represent the mean  $\pm$  SE of three experiments. \* $P < 0.01$  by the Student's *t*-test.

### Immunohistochemistry

Immunoperoxidase procedure was performed on the paraffin-embedded sections with standard avidin-

biotin-peroxidase complex method. After antigen retrieval with Pascal pressurized heating chamber (DAKO A/S, Glostrup, Denmark), the sections were incubated with anti-NR0B1 (Abcam; 1:100). As the negative control, staining was performed in the absence of primary antibody. Immunohistochemically stained sections were evaluated independently by two investigators (T. O. and E. M.); the results were compared and discussed for patients with discrepant findings.

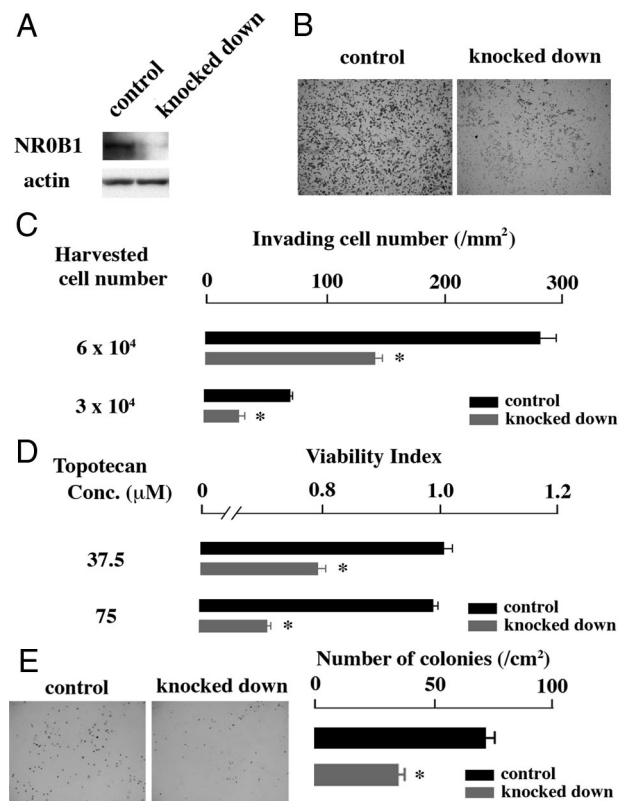


**Figure 5.** Effect of NR0B1 in PC-14. **A:** Immunoblot analysis for the amount of NR0B1 protein in the control and si-RNA knocked down PC-14 cells. **B:** Matrigel invasion assay using PC-14 cells. Cells invading through Matrigel were shown. Original magnification,  $\times 100$ . **C:** Invading cell number per mm<sup>2</sup>. **D:** Viability of PC-14 cells in the presence of topotecan was compared. **E:** Colonies derived from the control and the NR0B1 knocked down PC-14 cells, and the number of colonies per cm<sup>2</sup>. The values in (C), (D), and (E) represent the mean  $\pm$  SE of three experiments. \* $P < 0.01$  by the Student's *t*-test.

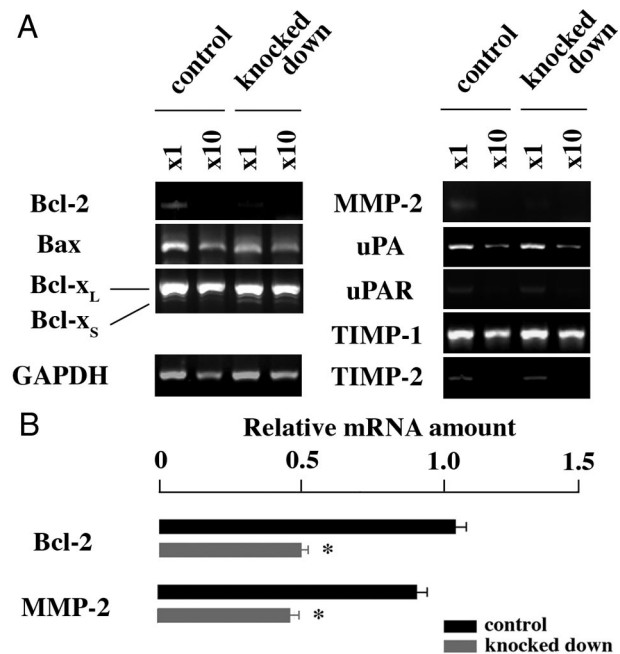


**Figure 6.** Expression of apoptosis- and invasion-related genes in NR0B1-knocked down A549 cells. **A:** Semiquantitative RT-PCR. **B:** Real-time quantitative RT-PCR to examine the expression level of Bcl-2 and MMP-2. The value is shown as the mean  $\pm$  SE. \* $P < 0.01$  by the Student's *t*-test.

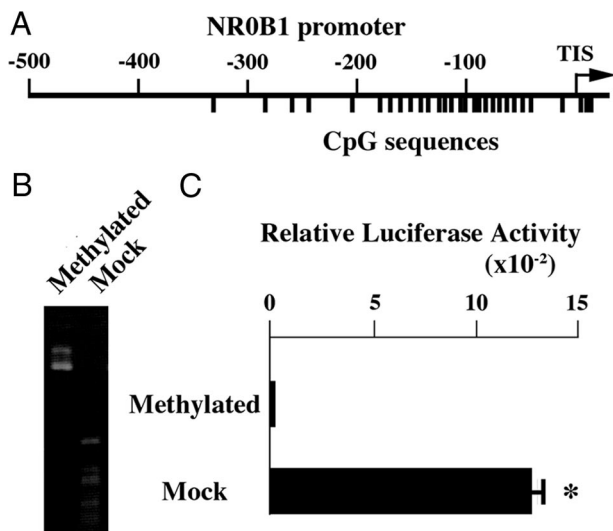


**Figure 7.** Effect of methylation on NR0B1 promoter activity. **A:** CpG sequences in the NR0B1 promoter. The vertical line represents a single CpG site. Transcription initiation site (TIS) is shown as **arrow**. **B:** Digestion patterns with the methylation-sensitive restriction enzyme HpaII of methylated and mock-methylated reporter plasmids. The luciferase reporter plasmid containing NR0B1 promoter was methylated or mock-methylated *in vitro*. Subsequently, each construct was digested with HpaII and electrophoresed. **C:** Relative luciferase activities of the methylated and mock-methylated NR0B1 constructs. The values represent the mean  $\pm$  SE of three experiments. \* $P < 0.01$  by the Student's *t*-test. The SE of the methylated construct was too small to be shown.

### Statistics

Statistical analysis for experimental studies was performed using Student's *t*-tests. The values are shown as the mean  $\pm$  SE of at least three experiments. Statistical analysis for clinical samples was performed using Stat-View software (SAS Institute Inc., Cary, NC). Five-year overall survival (OS) and disease-free survival (DFS) were calculated by the Kaplan-Meier method, and the differences in survival curves were analyzed by the log-rank test. Independent prognostic factors were analyzed by the Cox's proportional hazards regression model.

### Results

#### High Expression Level of NR0B1 in SP of A549 Cells and Effects of its Knocked-Down by si-RNA

To examine whether expression level of NR0B1 was higher in SP than in MP, A549 cells were stained with Hoechst-33342, and the SP and MP were independently sorted (Figure 1A). The expression level of NR0B1 was approximately three times higher in the SP than in the MP (Figure 1B). The expression level of NR0B1 was reduced by si-RNA, but did not significantly affect the proliferative activity and the proportion of SP among A549 cells (Figure 2, A–D). Whereas, the anti-cancer effect of topotecan, which is a topoisomerase I inhibitor and induces apoptosis in tumor cells, was stronger in knocked down cells than in control cells at the concentration of 37.5 and 75  $\mu$ mol/L (Figure 3A). In Matrigel invasion assay, the number of invading cells in

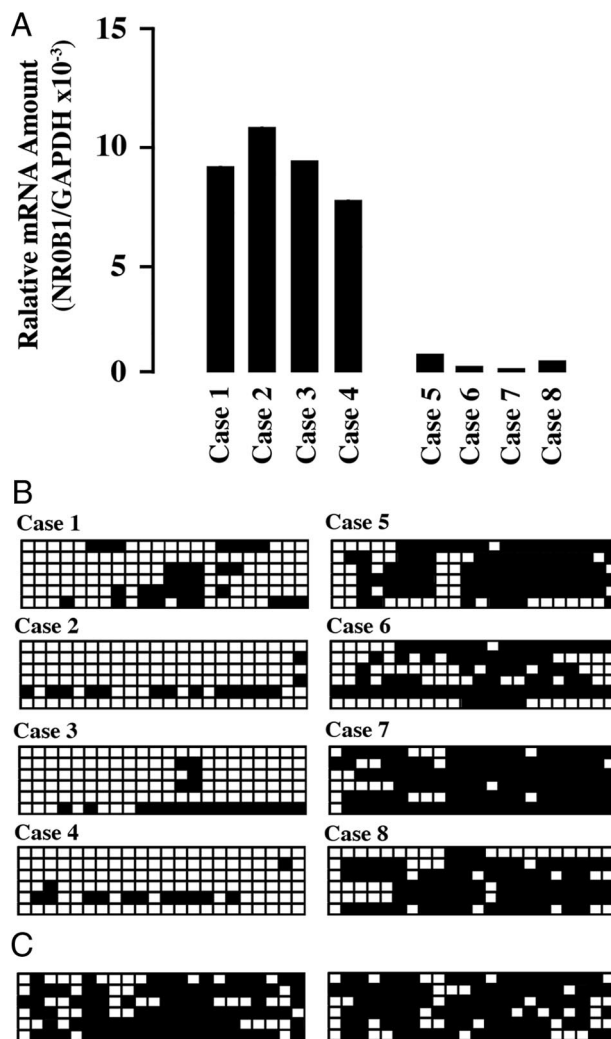


**Figure 8.** Inverse correlation of NR0B1 expression level to the proportion of methylated CpG sequences in clinical samples of lung adenocarcinoma. **A:** Quantitative real-time RT-PCR was performed with mRNA obtained from tumors. The amount of NR0B1 mRNA was normalized for the amount of GAPDH mRNA. The highest four and the lowest four cases were shown (cases 1 to 4, and cases 5 to 8, respectively). **B:** Methylation status of CpG sequences in NR0B1 promoter. Six clones for each population were analyzed by bisulfite sequencing. Open and closed squares denote unmethylated and methylated cytosines, respectively. **C:** Methylation status of CpG sequences in NR0B1 promoter of normal lung tissue from two cases.

knocked-down cells was lower than that of the control cells, indicating that the knocked-down expression of NR0B1 resulted in a defect of invasive ability (Figure 3, B and C).

#### Effect of NR0B1 on Colony Formation and Tumorigenic Abilities

The *in vitro* colony formation and *in vivo* tumorigenic activities of NR0B1 knocked-down cells were evaluated. As compared with the control cells, NR0B1 knocked-down cells formed lower number of colonies *in vitro* (Figure 4, A and B). When  $1 \times 10^4$  cells were injected into NOD/SCID mice, the size of tumors derived from NR0B1 knocked-down cells was significantly smaller than that of control cells (Figure 4, C and D). The tumor derived from either control or knocked-

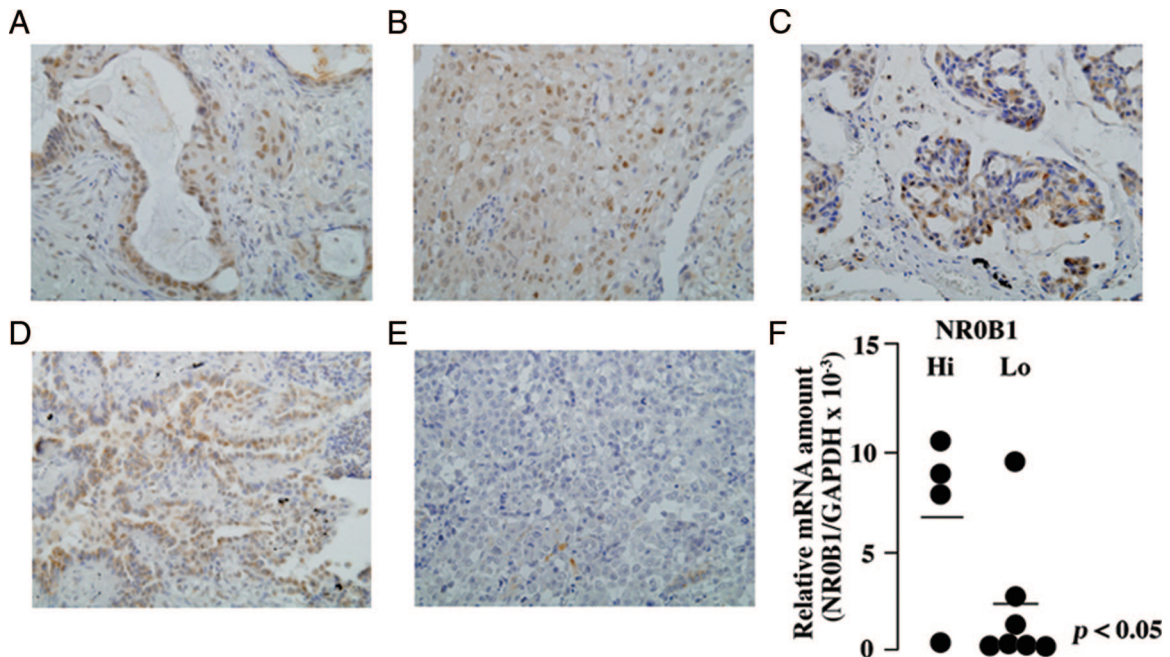


**Figure 9.** NR0B1 expression in clinical samples of lung adenocarcinoma. **A–E:** Representative pictures of NR0B1 immunostaining in various cases. ( $\times 400$ ) NR0B1 signals were detected in the nuclei of approximately 90% (**A**), 70% (**B**), 30% (**C**) of tumor cells. In some cases, the signals were detected not only in the nucleus but also in the cytoplasm (**D**). In other cases, few NR0B1-positive tumor cells were detected (**E**,  $<1\%$ ). **F:** Quantitative real-time RT-PCR was performed with mRNA obtained from 11 tumors as described in Figure 8A. The amount of NR0B1 mRNA was normalized for the amount of GAPDH mRNA. The amount of NR0B1 mRNA was higher in immunohistochemically defined NR0B1-hi cases than in NR0B1-lo cases. The bar shows mean value of NR0B1 amount.

down cells histologically showed glandular structures, mimicking lung adenocarcinoma (Figure 4E).

### Effect of NR0B1 in Another Lung Cancer Cell Line

To examine the effect of NR0B1 observed in A549 was applicable to another lung adenocarcinoma cell line, the

NR0B1 expression was knocked down in PC-14 (Figure 5A). Matrigel invasion assay revealed that the number of invading cells at NR0B1-knocked down condition reduced to half of the control cells (Figure 5, B and C). The anti-cancer effect of topotecan was stronger in knocked down cells than in control cells (Figure 5D). In addition, the *in vitro*-formed colony number derived from knocked down cells was smaller than that of control cells (Figure 5E).

**Table 1.** Brief Summary of 193 Patients with Pulmonary Adenocarcinoma

	No. of patients
Sex	
Male	107
Female	86
T Category	
1	130
2	45
3	13
4	5
N Category	
N0	160
N1	6
N2	24
N3	3
Stage	
I	145
II	18
III	30
Recurrence	
Yes	53
No	140
Prognosis	
Dead	37
Alive (with recurrence)	12
Alive (with no recurrence)	144

### Decreased Expression Level of Apoptosis- and Invasion-Related Genes in NR0B1 Knocked-Down Cells

To examine why the colony formation and invasion abilities were defective in NR0B1-knocked down cells, the expression level of apoptosis- and invasion-related genes (Bcl-2, Bax, Bcl-X<sub>L/S</sub>, MMP-2, uPA, uPA receptor, TIMP-1, and TIMP-2) was analyzed. Among the examined genes, Bcl-2 and MMP-2 expression levels were lower in knocked-down cells than in control cells (Figure 6A). Real-time quantitative RT-PCR revealed that the amount of Bcl-2 and MMP-2 mRNAs in knocked down cells decreased to half of control cells (Figure 6B).

### Epigenetic Regulation of NR0B1 Expression

A number of CpG sequences were found around the transcription initiation site of NR0B1 gene (Figure 7A), suggesting that the transcription of NR0B1 gene might be epigenetically regulated. To examine this, the luciferase construct containing NR0B1 promoter was methylated *in vitro* using SssI methylase, and the methylated or mock-

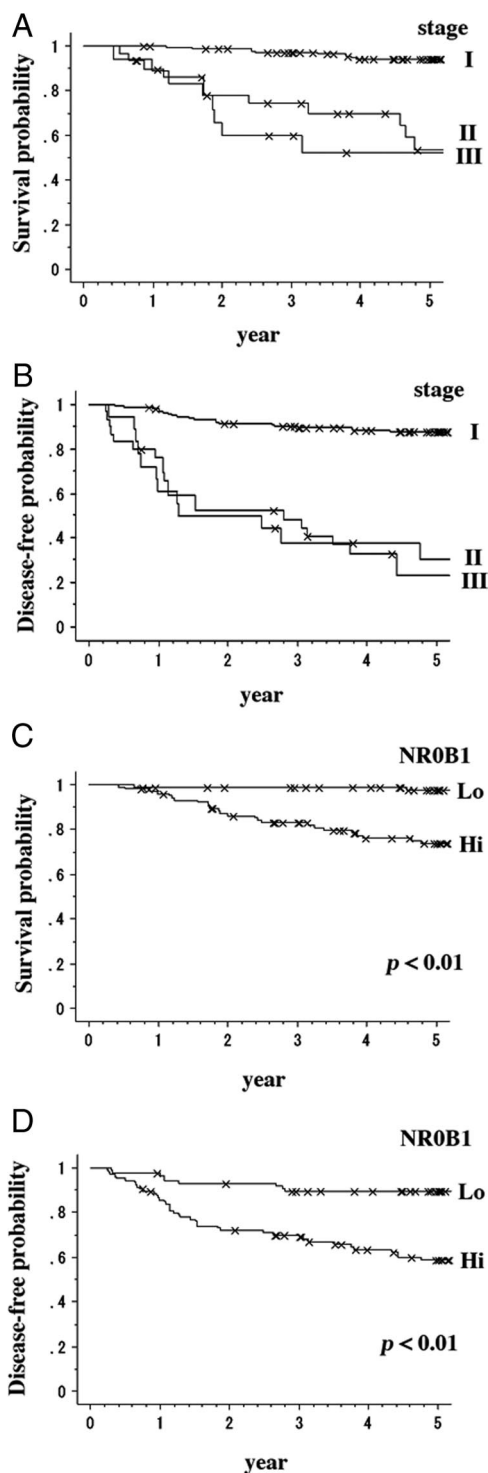


**Figure 10.** Relation of NR0B1 expression to prognosis of clinical cases. **A:** OS in 193 lung adenocarcinoma cases. Five-year OS in all patients, patients with stage I, II, and III was 84.8%, 95.1%, 52.4%, and 53.8%, respectively. **B:** Five year DFS in all patients, patients with stage I, II, and III was 73.1%, 87.9%, 30.5%, and 23.4%, respectively. OS (**C**) and DFS (**D**) curves in NR0B1-hi and NR0B1-lo cases.

methylated promoter construct was transiently transfected into A549. The methylated promoter construct, but not the mock-methylated construct, was resistant to digestion with methylation-sensitive restriction enzyme

**Table 2.** Correlation of NR0B1 Expression in Lung Adenocarcinoma with Clinicopathological Factors

	NR0B1		P value
	Hi	Lo	
T Category			0.855
1	73	57	
2	23	22	
3	7	6	
4	2	3	
N Category			0.021
N0	79	81	
N1	5	1	
N2	19	5	
N3	2	1	
Stage of disease			0.069
I	72	73	
II	12	6	
III	21	9	
Recurrence			<0.01
Yes	43	10	
No	62	78	

HpaII (Figure 7B), which confirmed that the CpG sequences of methylated construct had been completely methylated *in vitro*. When transfected into A549, higher luciferase activities were detected for the mock-methylated NR0B1 promoter than for the methylated NR0B1 promoter (Figure 7C).

Next, the correlation of methylated CpG proportion with NR0B1 expression level was analyzed in clinical samples of lung adenocarcinoma. The NR0B1 expression level in clinical samples was determined by quantitative real-time PCR. The genome DNA was extracted from each four case of lung adenocarcinoma showing high (Figure 8A, case 1 to case 4) and low level of NR0B1 expression (Figure 8A, case 5 to case 8). Bisulfite sequencing revealed that the proportion of methylated CpG sites was lower in cases with high NR0B1 expression than in cases with low NR0B1 expression (Figure 8B). The proportion of methylated CpG sites was high in the normal lung tissue (Figure 8C).

### Immunohistochemical Analysis of NR0B1 Expression in Lung Adenocarcinoma

Correlation of NR0B1 expression with clinicopathological findings was examined in clinical samples of lung adenocarcinoma. At immunohistochemistry, signals for NR0B1 were detected in cancerous lesions but not in the non-cancerous lesions. The subcellular localization of NR0B1 signals was detected mainly in the nuclei of adenocarcinoma cells in some cases (Figures 9, A–C), but detected not only in the nucleus but also in the cytoplasm in others (Figure 9D); nuclear staining pattern in 27 cases, cytoplasmic pattern in 25 cases, and nucleocytoplasmic pattern in 53 cases. Few signals could be detected in several cases (Figure 9E). According to the method by Saito et al,<sup>26</sup> a total of more than 500 tumor cells from three different representative fields were examined, and the proportion of cells with NR0B1 signals was counted. The previous reports on NR0B1 expression



**Table 3.** Univariate and Multivariate Analysis of Prognostic Factors for Overall and Disease-Free Survivals

	OS				DFS			
	Univariate HR (95% CI)	P value	Multivariate HR (95% CI)	P value	Univariate HR (95% CI)	P value	Multivariate HR (95% CI)	P value
Age	1.001 (0.964–1.040)	0.961			0.992 (0.963–1.021)	0.566		
Sex	0.837 (0.413–1.698)	0.623			0.795 (0.458–1.379)	0.414		
T Category	2.005 (1.436–2.800)	<0.01	1.362 (0.809–2.291)	0.245	1.830 (1.393–2.403)	<0.01	1.078 (0.687–1.690)	0.744
N Category	2.442 (1.796–3.322)	<0.01	0.657 (0.306–1.411)	0.282	2.408 (1.888–3.072)	<0.01	0.768 (0.418–1.411)	0.395
Stage	2.982 (2.062–4.312)	<0.01	3.098 (1.187–8.084)	0.021	2.959 (2.220–3.944)	<0.01	2.825 (1.350–5.913)	<0.01
Tumor size	1.046 (1.025–1.066)	<0.01	1.029 (1.004–1.055)	0.021	1.041 (1.026–1.057)	<0.01	1.025 (1.005–1.045)	0.014
NROB1 level	0.083 (0.025–0.281)	<0.01	0.043 (0.009–0.195)	<0.01	0.208 (0.103–0.420)	<0.01	0.176 (0.078–0.397)	<0.01

HR, hazard ratio; CI, confidence interval; OS, overall survival; DFS, disease-free survival.

in endometrial adenocarcinoma<sup>26</sup> and prostatic carcinoma<sup>28</sup> used a cut-off point of 10%. Therefore, in this study, we used the same cut-off point; the cases with more than 10% positive cells and fewer than 10% positive cells were defined as NROB1-hi and NROB1-lo, respectively.

To confirm the specificity of immunohistochemical staining for NROB1 expression, quantitative real-time RT-PCR was performed on 11 cases with lung adenocarcinoma from which mRNA could be obtained (4 NROB1-hi and 7 NROB1-lo cases at immunohistochemical results). The amount of NROB1 mRNA was significantly higher in cases with NROB1-hi expression at immunohistochemistry than those with NROB1-lo expression ( $P < 0.05$ , Figure 9F). These results showed that the immunohistochemical evaluation is a reliable method for evaluation of NROB1 expression.

Brief clinical findings of 193 cases are summarized in Table 1. There were 107 males and 86 females with ages ranging from 33 to 82 (median, 64) years. Size of the main tumor ranged from 8 to 80 (median, 20) mm. Stage of tumor was I in 145 patients, II in 18, and III in 30. Tumor recurrence was found in 53 cases with intervals from surgery ranging from 2.9 to 145.3 (median 15.2) months. Five year OS in all patients, patients with stage I, II, and III was 84.8%, 95.1%, 52.4%, and 53.8%, respectively (Figure 10A). DFS in all patients, patients with stage I, II, and III was 73.1%, 87.9%, 30.5%, and 23.4%, respectively (Figure 10B).

Among 193 lung adenocarcinoma cases, 105 cases (54.4%) were categorized as NROB1-hi, and the remaining cases as NROB1-lo. Correlation of NROB1 expression level with clinical findings is shown in Table 2. The  $\chi^2$  analysis revealed that the N category and tumor recurrence significantly correlated with high NROB1 expression. Patients with NROB1-lo tumor showed significantly better OS and DFS than those with NROB1-hi tumors ( $P < 0.01$ , respectively) (Figure 10, C and D).

Univariate analysis revealed that high T category, lymph node metastasis (high N category), advanced stage, large tumor size, and high NROB1 expression were significant unfavorable factors for both 5-year OS and DFS (Table 3). Multivariate analysis revealed that the advanced stage, large tumor size, and high NROB1 expression were independent prognostic factors for both 5-year OS and DFS (Table 3).

## Discussion

Patient characteristics such as gender, age, and 5-year OS in the present study were similar to those in the previous reports.<sup>37</sup> In addition, the uni- and multivariate analyses showed the prognostic significance of clinicopathological factors, including tumor size and stage of disease, as reported previously.<sup>37</sup> These findings indicate that the results obtained from the present clinical cases are commonly applicable.

CSCs are known to be enriched in SP,<sup>17,20</sup> therefore proteins highly expressed in SP may become a candidate for CSC markers. Since the expression level of NROB1 is higher in SP than in MP of lung adenocarcinoma cell line, NROB1 might be further investigated as a candidate marker for CSCs of lung adenocarcinoma. The knocked down expression of NROB1 resulted in the decrease of resistance against topotecan, Matrigel invasion, *in vitro* colony formation, and *in vivo* tumorigenic activities. The involvement of NROB1 in the resistance against anti-cancer drugs and the high tumorigenicity was consistent with the higher rates of recurrence in the cases with NROB1-hi than those with NROB1-lo expression as shown in the clinical samples. In addition to recurrence, NROB1-hi tumors showed the higher frequency of lymph node metastasis than that of NROB1-lo tumors. Invasion of cancer cells into the surrounding tissues and high tumorigenic potential, which were characteristic to NROB1-high population, are essential for the establishment of lymph node metastasis.<sup>38,39</sup> Since NROB1 is not expressed on the cell surface, the sorting of NROB1-hi and NROB1-lo populations in living cells is impossible. Because the experiment to examine whether NROB1-hi, but not NROB1-lo, gives rise to both NROB1-hi and -lo populations is not possible due to above-mentioned reason, it is difficult to assess directly whether NROB1-hi population was CSCs or not. Still, the involvement of NROB1 in the resistance against anti-cancer drug, invasiveness, and high tumorigenic potentials in A549 and PC-14 cell lines suggested that NROB1 might be candidate marker for CSCs, or at least, for tumorigenic cells of lung adenocarcinoma.

Kinsey et al<sup>30</sup> and Garcia-Aragoncillo et al<sup>40</sup> reported that NROB1 expression is related to cell proliferative activity in Ewing's sarcoma cell lines. In contrast, the knocked-down expression of NROB1 did not affect the

cell proliferation of A549 cells. This might be attributable to the difference of cell types; Saito et al<sup>26</sup> and Nakamura et al<sup>28</sup> did not find any correlation of NROB1 expression level with the Ki-67 labeling index, a well-established marker for cell proliferative activity, in the endometrial adenocarcinoma of uterus and prostate. The present study on the clinical cases of lung adenocarcinoma showed that NROB1 expression level did not correlate with the size of tumors. NROB1 appeared to play a role for cell proliferation in Ewing's sarcoma but not in lung, endometrial, and prostatic adenocarcinomas.

The knocked down expression of NROB1 had no effect on cell growth (assessed by cell number), but significantly affected tumorigenic and invasion abilities. The expression level of MMP-2 decreased in knocked-down cells, which may explain the low invasion ability. The defective anti-apoptotic ability of knocked-down cells as revealed decreased expression of Bcl-2 might explain the normal proliferation potential (cell growth), but low tumorigenicity. NROB1 is reported to antagonize several transcription factors, including WT-1,<sup>41</sup> which is known to suppress Bcl-2 promoter.<sup>42</sup> NROB1 might antagonize the function of WT-1, thereby enhancing Bcl-2 transcription. Although the precise mechanism remains to be clarified, the defective expression of Bcl-2 and MMP-2 could be causative for the low tumorigenic and invasion abilities of NROB1 knocked-down cells.

The formation of SP was found even when the expression of NROB1 was reduced, indicating that NROB1 was not necessary for SP formation. For SP formation, several chemical transporters, such as ABCG2, are involved.<sup>15–17</sup> NROB1 might not affect the expression of these chemical transporters.

In adenocarcinoma of uterine endometrium and prostate, NROB1 was present in the nucleus, but not in the cytoplasm.<sup>26,28</sup> Whereas, the subcellular localization of NROB1 was various among cases with the present lung adenocarcinoma. Kawajiri et al<sup>43</sup> reported that NROB1 localization changed during pituitary development from nucleocytoplasmic at embryonic day 10.5 to nucleus at day 18.5. Helguero et al<sup>44</sup> demonstrated that NROB1 localized in the nucleus of mammary gland in virgin mice, nucleocytoplasmic in pseudopregnant mice, and cytoplasmic in lactating mice. To date, the functional heterogeneity of NROB1 depending on the subcellular localization has not been clarified. Although no significant differences in clinicopathological findings were found among cases with these three staining patterns, further analysis with a larger number of cases is necessary to reveal the functional heterogeneity of NROB1 depending on the subcellular localization.

Numerous CpG sequences around the NROB1 promoter suggested the epigenetic regulation of its transcription. In fact, the promoter activity of NROB1 significantly decreased when the CpG sequences were methylated *in vitro*. The proportion of CpG methylation was inversely correlated with the NROB1 expression level in clinical samples. Very recently, Garcia-Aragoncillo et al<sup>40</sup> reported that EWS/FLI1 directly binds to the GGAA-rich region in NROB1 promoter and transactivates its activity. It is well known that transcription factors may

bind to their cognate recognition sequences when the promoter region is relaxed in the unmethylated state.<sup>45</sup> The promoter region of NROB1 in Ewing's sarcoma appeared to be relaxed, whereas in lung adenocarcinoma it possesses a packed promoter in the heavily methylated condition. Demethylation may enable some unknown transcription factors to bind and transactivate NROB1 promoter in lung adenocarcinoma. Further studies are needed to clarify such transcription factors.

Taken together, NROB1 was involved in resistance against anti-cancer drugs, invasion, *in vitro* colony formation, and *in vivo* tumorigenic potentials of lung adenocarcinoma cell line. NROB1-hi cases showed the higher frequency of lymph node metastasis and tumor recurrence than those of NROB1-lo cases. The high level of NROB1 expression was an independent poor prognostic factor in the cases with lung adenocarcinoma.

### Acknowledgments

We thank Ms. Megumi Sugano, Ms. Etsuko Maeno, and Ms. Takako Sawamura for their technical assistance.

### References

1. Heppner GH: Tumor heterogeneity. *Cancer Res* 1984, 44:2259–2265
2. Hemburger AW, Salmon SE: Primary bioassay of human tumor stem cells. *Cell Sci* 1977, 197:461–463
3. Bruce WR, Van Der Gaag H: A quantitative assay for the number of murine lymphoma cells capable of proliferation *in vivo*. *Nature* 1963, 199:79–80
4. Reya T, Morrison SJ, Clarke MF, Weissman IL: Stem cells, cancer, and cancer stem cells. *Nature* 2001, 414:105–111
5. Bonnet D, Dick JE: Human acute myeloid leukemia is organized as a hierarchy that originates from a primitive hematopoietic cell. *Nat Med* 1997, 3:730–737
6. Lessard J, Sauvageau G: Bmi-1 determined the proliferative capacity of normal and leukaemic stem cells. *Nature* 2003, 423:255–260
7. Al-Hajj M, Wicha MS, Benito-Hernandez A, Morrison SJ, Clarke MF: Prospective identification of tumorigenic breast cancer cells. *Proc Natl Acad Sci USA* 2003, 100:3983–3988
8. Singh SK, Hawkins C, Clarke ID, Squire JA, Bayani J, Hide T, Henkelman RM, Cusimano MD, Dirks PB: Identification of human brain tumour initiating cells. *Nature* 2004, 432:396–401
9. Collins AT, Berry PA, Hyde C, Stower MJ, Maitland NJ: Prospective identification of tumorigenic prostate cancer stem cells. *Cancer Res* 2005, 65:10946–10951
10. O'Brien CA, Pollett A, Gallinger, Dick JE: A human colon cancer cell capable of initiating tumor growth in immunodeficient mice. *Nature* 2007, 445:106–110
11. Ricci-Vitiani L, Lombardi DG, Pilozzi E, Biffoni M, Todaro M, Peschle C, DeMaria R: Identification and expansion of human colon-cancer-initiating cells. *Nature* 2007, 445:111–115
12. Prince ME, Sivanandan R, Kaczorowski, Wolf GT, Kaplan MJ, Dalerba P, Weissman IL, Clarke MF, Ailles LE: Identification of a subpopulation of cells with cancer stem cell properties in head and neck squamous cell carcinoma. *Proc Natl Acad Sci USA* 2007, 104: 973–978
13. Li C, Heidt DG, Dalerba P, Burant CF, Zhang L, Adsav V, Wicha M, Clarke MF, Simeone DM: Identification of pancreatic cancer stem cells. *Cancer Res* 2007, 67:1030–1037
14. Dean M, Fojo T, Bates S: Tumor stem cells and drug resistance. *Nat Rev Cancer* 2005, 5:275–284
15. Lou H, Dean M: Targeted therapy for cancer stem cells: the patched pathway and ABC transporters. *Oncogene* 2007, 26:1357–1360
16. Goodell MA, Brose K, Paradis G, Conner AS, Mulligan RC: Isolation

- and functional properties of murine hematopoietic stem cells that are replicating in vivo. *J Exp Med* 1996, 183:1797–1806
17. Hadnagy A, Gaboury L, Beaulieu R, Balicki D: SP analysis may be used to identify cancer stem cell populations. *Exp Cell Res* 2006, 14:387–391
  18. Kondo T, Setoguchi T, Taga T: Persistence of a small subpopulation of cancer stem-like cells in the C6 glioma cell line. *Proc Natl Acad Sci USA* 2004, 101:781–786
  19. Setoguchi T, Taga T, Kondo T: Cancer stem cells persist in many cancer cell lines. *Cell Cycle* 2004, 3:414–415
  20. Patrawala L, Calhoun T, Schneider-Broussard R, Li H, Bhatia B, Tang S, Reilly JG, Chandra D, Zhou J, Claypool K, Coghlan L, Tang DG: Side population is enriched in tumorigenic, stem-like cancer cells, whereas ABCG2+ and ABCG2- cancer cells are similarly tumorigenic. *Cancer Res* 2005, 65:6207–6219
  21. Parkin DM, Bray F, Ferlay J, Pisani P: Global Cancer Statistics, 2002. *CA Cancer J Clin* 2005, 55:74–108
  22. Seo DC, Sung JM, Cho HJ, Yi H, Seo KH, Choi IS, Kim DK, Kim JS, El-Aty AMA, Shin HC: Gene expression profiling of cancer stem cell in human lung adenocarcinoma A549 cells. *Mol Cancer* 2007, 6:75
  23. Niakan KK, McCabe ER: DAX1 origin, function, and novel role. *Mol Genet Metab* 2005, 86:70–83
  24. Palmqvist L, Glover CH, Hsu L, Bossen B, Piret JM, Humphries RK, Helgason CD: Correlation of murine embryonic stem cell gene expression profiles with functional measures of pluripotency. *Stem Cells* 2005, 23:663–680
  25. Niakan KK, Davis EC, Clipsham RC, Jiang M, Dehart DB, Sulik KK, McCabe ER: Novel role for the orphan nuclear receptor DAX1 in embryogenesis different from steroidogenesis. *Mol Genet Metab* 2006, 88:261–271
  26. Saito S, Ito K, Suzuki T, Utsunomiya H, Akahira JI, Sugihashi Y, Niikura H, Okamura K, Yaegashi N, Sasano H: Orphan nuclear receptor DAX-1 in human endometrium and its disorders. *Cancer Sci* 2005, 96:645–652
  27. Abd-Elaziz M, Akahira J, Moriya T, Suzuki T, Yaegashi N, Sasano H: Nuclear receptor DAX-1 in human common epithelial ovarian carcinoma: an independent prognostic factor of clinical outcome. *Cancer Sci* 2003, 94:980–985
  28. Nakamura Y, Suzuki T, Arai Y, Sasano H: Nuclear receptor DAX1 in human prostate cancer: a novel independent biological modulator. *Endocr J* 2009, 56:39–44
  29. Mendiola M, Carrillo J, García E, Lalli E, Hernández T, de Alava E, Tirode F, Delattre O, García-Miguel P, López-Barea F, Pestaña A, Alonso J: The orphan nuclear receptor DAX1 is up-regulated by the EWS/FLI1 oncoprotein and is highly expressed in Ewing tumors. *Int J Cancer* 2006, 118:1381–1389
  30. Kinsey M, Smith R, Lessnick SL: NROB1 is required for the oncogenic phenotype mediated by EWS/FLI in Ewing's sarcoma. *Mol Cancer Res* 2006, 4:851–859
  31. Morii E, Oboki K, Jippo T, Kitamura Y: Additive effect of mouse genetic background and mutation of MITF gene on decrease of skin mast cells. *Blood* 2003, 101:1344–1350
  32. Slichenmyer WJ, Von Hoff DD: New natural products in cancer chemotherapy. *J Clin Pharmacol* 1990, 30:770–788
  33. Tomacic MT, Christmann M, Kaina B: Topotecan-triggered degradation of topoisomerase I is p53-dependent and impacts cell survival. *Cancer Res* 2005, 65:8920–8926
  34. Meyer-Siegler KL, Iczkowski KA, Leng L, Bucala R, Vera PL: Inhibition of macrophage migration inhibitory factor or its receptor (CD74) attenuates growth and invasion of DU-145 prostate cancer cells. *J Immunol* 2006, 177:8730–8739
  35. Guo W, Burris TP, Zhang YH, Huang BL, Mason J, Copeland KC, Kupfer SR, Pagon RA, McCabe ERB: Genomic sequence of the DAX1 gene: an orphan nuclear receptor responsible for X-linked adrenal hypoplasia congenital and hypogonadotropic hypogonadism. *J Clin Endocrinol Metab* 1996, 81:2481–2486
  36. Sobin LH, Wittekind Ch (Eds.): TNM Classification of malignant tumors. 5th ed. New York, John Wiley & Sons, Inc., 1997, pp 91–100
  37. Suzuki K, Nagai K, Yoshida J, Nishimura M, Takahashi K, Yokose T, Nishiwaki Y: Conventional clinicopathologic prognostic factors in surgically resected nonsmall cell lung carcinoma. *Cancer* 1999, 86:1976–1984
  38. Li F, Tiede B, Massague J, Kang Y: Beyond tumorigenesis: cancer stem cells in metastasis. *Cell Res* 2007, 17:3–14
  39. Brabletz T, Jung A, Spaderna S, Hlubek F, Kirchner T: Opinion: migrating cancer stem cells—an integrated concept of malignant tumor progression. *Nat Rev Cancer* 2005, 5:744–749
  40. García-Aragoncillo E, Carrillo J, Lalli E, Agra N, Gómez-López G, Pestaña A, Alonso J: DAX1, a direct target of EWS/FLI1 oncoprotein, is a principal regulator of cell-cycle progression in Ewing's tumor cell. *Oncogene* 2008, 27:6034–6043
  41. Lalli E, Sassone-Corsi P: Dax-1, an unusual orphan receptor at the crossroads of steroidogenic function and sexual differentiation. *Mol Endocrinol* 2003, 17:1445–1453
  42. Hewitt SM, Hamada S, McDonnell TJ, Rauscher FJ 3rd, Saunders GF: Regulation of the proto-oncogenes bcl-2 and c-myc by the Wilms tumor suppressor gene WT1. *Cancer Res* 1995, 55:5386–5389
  43. Kawajiri K, Ikuta T, Suzuki T, Kusaka M, Muramatsu M, Fujieda K, Tachibana M, Morohashi K: Role of the LXXLL-motif and activation function 2 domain in subcellular localization of Dax-1. *Mol Endocrinol* 2003, 17:994–1004
  44. Helguero LA, Hedengran Faulds M, Förster C, Gustafsson JA, Haldosén LA: DAX-1 expression is regulated during mammary epithelial differentiation. *Endocrinology* 2006, 147:3249–3259
  45. Feinberg AP, Tycko B: The history of cancer epigenetics. *Nat Rev Cancer* 2004, 4:143–153